The Specific Characteristics of Surface Heat Islands in Semi-Arid Environments. Implications for Urban and Landscape Planning

Francesca Miccoli(✉), Antonio Leone, and Antonella Longo

University of Salento, 73100 Lecce, Italy
francesca.miccoli@unisalento.it

Abstract. Urban thermal patterns are shaped by a combination of land-cover configuration, surface energy exchanges and regional climatic drivers. Although the classical Surface Urban Heat Island (SUHI) paradigm describes urban areas as warmer than their surrounding rural environments, recent studies, conducted in arid and semi-arid regions, have reported the occurrence of daytime cooling effects within urban areas, commonly referred to as the Surface Urban Cool Island (SUCI) phenomenon.

This study examines summer Land Surface Temperature (LST) dynamics in the municipality of Lecce (Southern Italy), a Mediterranean city, characterized by hot, dry summers and peri-urban agricultural landscapes under seasonal water stress. LST was retrieved from Landsat 8/9 TIRS imagery (June-August 2024, cloud cover $< 10\%$), using the Single Channel Algorithm applied to Band 10. To establish a rural thermal reference, a spatial filtering was applied within a buffer of 5–10 km from the urban centroid. Corine Land Cover data were used to exclude anthropogenic surface and water bodies, as well as to identify thermally anomalous areas. Thermal anomalies (ΔT) were then calculated relative to the filtered rural reference.

Results reveal an inversion of the classical Surface Urban Heat Island (SUHI) pattern during late-morning satellite acquisition ($\approx$11:30 local time). The historic urban core shows negative thermal anomalies (down to -4.87 °C) compared to the surrounding peri-urban agricultural matrices. Thermal hotspots were primarily concentrated in non-irrigated croplands, bare soils, olive groves affected by water stress and industrial areas. These findings indicate that, under summer semi-arid conditions, peri-urban soils act as thermally dominant sensible heat sources, whereas urban morphology and material properties induce a transient daytime SUCI effect.

This study integrates urban climatology and soil degradation perspectives within a unified surface energy balance framework, highlighting the climatic dependency of urban thermal regimes in Mediterranean transitional environments.

Keywords: Urban Heat and Cool Island · Land Surface Temperature · Landsat images · Planning

© The Author(s), under exclusive license to Springer Nature Switzerland AG 2027
O. Gervasi et al. (Eds.): ICCSA 2026 Workshops, LNCS 16762, pp. 3–20, 2027.
https://doi.org/10.1007/978-3-032-30524-4_1

1 Introduction

1.1 The Heat Island Issue

Urbanization represents one of the most pervasive anthropogenic transformations of the Earth's surface, profoundly altering land-atmosphere energy exchanges [1]. Among its most documented climatic impacts is the Urban Heat Island (UHI) phenomenon, defined as the thermal contrast between urban areas and their rural surroundings [2]. Traditionally, UHI has been investigated in terms of canopy air temperature [3], whereas the advent of thermal remote sensing has enabled the assessment of the Surface Urban Heat Island (SUHI) through Land Surface Temperature (LST) measurements [4–6].

LST acts as a primary indicator of the surface energy balance [7]. Urban expansion has drastically modified land cover [8], replacing natural landscapes with impervious surfaces, characterized by high thermal mass and lower albedo compared to rural agricultural or forested areas [2]. This alters both the hydrological cycle and the distribution of incident solar radiation [9]. Focusing on climatic impacts, soil sealing causes the rapid discharge of runoff during precipitation events, thereby reducing evapotranspiration [9]. Simultaneously, construction materials, featuring high heat capacity, combined with compact urban geometry, trap incoming radiation within urban canyons [10, 11]. This elevates the LST without significant latent heat dissipation [4, 12].

Thermal remote sensing has proven fundamental in the systematic, multi-scale monitoring of surface thermal anomalies [4, 13, 14]. Recently, the availability of satellite platforms equipped with Thermal Infrared (TIR) sensors, such as Landsat 8 and 9, MODIS, ASTER, Sentinel-3, and ECOSTRESS, has advanced SUHI research [15, 16]. The choice of sensors entails a methodological trade-off: although instruments like Sentinel-3 or ECOSTRESS provide high temporal resolution, which is ideal for studying diurnal and nocturnal cycles [17], the TIRS sensors aboard the Landsat constellation remain among the most suitable for intra-urban spatial analyses [18–21]. Despite being limited by a 16-day revisit time, their 100 m spatial resolution, resampled to 30 m, allows for precise mapping of the interactions between urban morphology and temperature [22]. For LST retrieval, the Single Channel Algorithm (SCA) has been extensively validated for Landsat 8 TIRS data, proving optimal when applied to Band 10 due to its greater radiometric stability [23, 24].

1.2 Urban Heat, Soil Degradation and Shared Energetic Drivers

Parallel to UHI research, an extensive literature has addressed soil degradation processes, both broadly [25] and specifically within Mediterranean and semi-arid environments [18, 26], highlighting their direct impacts on desertification [27, 28]. Erosion, loss of vegetative cover, and intensive agricultural practices, particularly deep plowing and soil compaction, alter soil properties under already critical climatic conditions [29].

These intensive practices deplete Soil Organic Carbon (SOC) [25, 30], which in turn alters soil properties. This depletion reduces heat capacity, bringing the thermal inertia of dehydrated agricultural soil closer to that of construction materials [31] and diminishing water retention [32]. These physical changes increase the dominance of sensible heat fluxes during dry seasons, consequently raising surface temperatures [27, 33].

Research rarely addresses UHI and soil degradation in an integrated manner, although these processes share common physical drivers and impacts, such as reduced evaporative cooling, increased surface exposure, and altered radiative properties. Under summer semi-arid conditions, non-irrigated agricultural soils can reach surface temperatures exceeding those of adjacent urban centers, particularly during morning and afternoon observations [34, 35]. This dynamic challenges the classical paradigm that views urban cores as systematically warmer than rural areas, an issue warranting further investigation to which this paper aims to provide an initial contribution.

1.3 Urban Cool Island and Climatic Dependency of Thermal Gradients

Recent studies conducted in arid and desert environments have documented a diurnal reversal of the conventional UHI signal, introducing the concept of the Urban Cool Island (UCI) [6, 14, 34, 35]. In such contexts, barren or sparsely vegetated rural surfaces undergo rapid radiative heating due to low thermal inertia and severely limited evapotranspiration [6, 18, 35–37]. Conversely, compact urban grids frequently record lower daytime LSTs. Vertical shading within urban canyons, the high thermal mass of construction materials, and localized irrigated vegetation all drive this temporary cooling effect [6, 19, 31, 34, 38, 39].

Analyzing over 100 cities in arid and semi-arid climates globally, Liu et al. (2024) [14] demonstrated that the daytime UCI phenomenon is a frequent occurrence, observed in approximately 50% of the sampled locations. The literature offers several examples of this anomaly: Gago et al. (2020) [40] analyzed Landsat-derived LST for the city of Seville (Spain) over a three-decade timeframe, revealing that urban areas remain cooler than surrounding bare soils and agricultural lands during dry summer periods. Abedrabboh et al. (2025) [6] documented a similar phenomenon in Smara (Morocco), recording a daytime UCI of up to 9 °C, largely driven by the strong albedo contrast between the dark desert lands and the urban core characterized by light-colored surfaces. Further supporting this, Siddiqui et al. (2025) [34] observed a daytime UCI of 3.5–4.6 °C in Erbil (Iraq), attributing the thermal dampening to urban density and water bodies contrasting with the arid outskirts.

1.4 Research Gap and Study Objective

Mediterranean climates, classified as Csa under the Köppen system, feature hot, dry summers and marked seasonal water deficits. During the summer, peri-urban agricultural landscapes, dominated by non-irrigated crops or bare soils, act thermally like semi-arid systems. Under these conditions, rural matrices exhibit a low evaporative fraction, high sensible heat flux dominance and rapid diurnal heating.

Concurrently, historic urban cores, characterized by a low Sky View Factor (SVF), shade and thermally insulate the urban grid during the morning. This delays surface temperature peaks, generating a temporary daytime cool island effect. Despite this emerging evidence, Mediterranean cities remain noticeably underrepresented in studies tracking the diurnal transition from UHI to UCI. This gap is particularly concerning given the accelerating regional trends of soil drying and climate change.

Therefore, this study aims to:

1. quantify high spatial resolution summer LST patterns within the municipality of Lecce (Southern Italy);
2. establish a robust rural thermal baseline using rigorous land-cover spatial filtering;
3. assess the occurrence, spatial extent and intensity of the daytime UCI effect;
4. examine the physical relationship between peri-urban thermal hotspots and localized soil degradation processes.

By linking urban climatology with land degradation research, this work refines the conceptual understanding of climate-dependent urban thermal regimes. It provides empirical evidence to reinterpret summer Mediterranean dynamics within a semi-arid energetic framework.

2 Materials and Methods

The investigation focuses on the municipality of Lecce (Southern Italy, see Fig. 1), situated in the Salento peninsula. The climate is typically Mediterranean (Köppen classification: Csa; source: https://koeppen-geiger.vu-wien.ac.at/), with hot, dry summers and mild, wetter winters.

The urban fabric is characterized by a compact historic center with narrow streets and high height-to-width (H/W) ratios, surrounded by peri-urban agricultural landscapes dominated by non-irrigated arable lands and olive groves.

The summer of 2024 was selected for this analysis due to its persistent high solar irradiance and cumulative precipitation deficit. These meteorological conditions strongly amplify surface thermal contrasts [41, 42].

To assess the dynamics of both the Surface Urban Heat Island (SUHI) and the Surface Urban Cool Island (SUCI), Land Surface Temperature (LST) was retrieved using Thermal Infrared (TIR) sensors. Although several consolidated algorithms exist for LST retrieval, such as the Radiative Transfer Equation (RTE) and the Split-Window Algorithm (SWA) [24], the Single Channel Algorithm (SCA) was selected [23].

For intra-urban analyses, involving high morphological heterogeneity, literature favors Landsat TIRS data resampled to a 30 m spatial resolution over coarser sensors like MODIS (1 km) [19], despite the higher temporal frequency of the latter. Choosing Landsat represents a compromise between spatial resolution (30 m for multispectral, 100 m for TIR resampled to 30 m), temporal revisit time (16 days per single satellite) and radiometric accuracy (12-bit, scaled to 16-bit in distributed products) [43, 44].

In this study, LST dynamics were investigated using data acquired by the TIRS sensors onboard Landsat 8 and TIRS-2 onboard Landsat 9. These sensors are widely utilized and validated for urban thermal mapping [20, 22–24, 45]. For the Lecce case study, summer scenes between June 1, 2024 and September 1, 2024, were acquired, strictly filtering for cloud cover below 10% (9 scenes in total). This specific temporal window was defined based on a meteorological analysis using data provided by the regional environmental agency ARPA portal (source: http://www.webgis.arpa.puglia.it/meteo/).

This period exhibited a severe radiative load (average seasonal solar irradiance of 283.30 W/m2) combined with a cumulative rainfall deficit. Under these specific conditions, both heat island phenomena and soil water stress become highly pronounced.

A critical factor, for correctly interpreting the data, is the Landsat satellite overpass time, which occurs at approximately 09:30 UTC (11:30 local time). This late-morning window captures the active phase of surface thermal accumulation and the specific shadowing dynamics of the urban geometry, playing a decisive role in defining the observed spatial patterns.

LST data for the Lecce municipality were derived from the Landsat Collection 2 Level-2 Surface Temperature (L2SP) product, provided by the USGS (source: https://earthexplorer.usgs.gov/). Relying on this Level-2 product eliminates the uncertainties typically associated with manual atmospheric corrections required for Level-1 data. The L2SP algorithm implements the SCA on Band 10, correcting atmospheric effects by integrating the Radiative Transfer Equation (RTE). It utilizes atmospheric profiles extracted from the NASA Earth Observing System for Instrument Teams (GEOS-IT) to accurately calculate atmospheric transmittance, upwelling radiance and downwelling radiance. Furthermore, surface emissivity (ε) is incorporated via the ASTER Global Emissivity Dataset (GED). Excluding Band 11 is due to documented residual calibration issues, primarily stray light artifacts [44].

Final LST values (in degrees Celsius) were obtained by applying the Collection 2 scale factors to the pre-processed pixel thermal values (DN_{ST}):

$$LST(\circ C) = [(DN_{ST} \times M_T) + A_T] - 273.15 \quad (1)$$

Here, DN_{ST} represents the pre-processed pixel Digital Number, while M_T and A_T define the multiplicative scale factor and additive scale factor, respectively, extracted from the _MTL.txt metadata file accompanying each image [45].

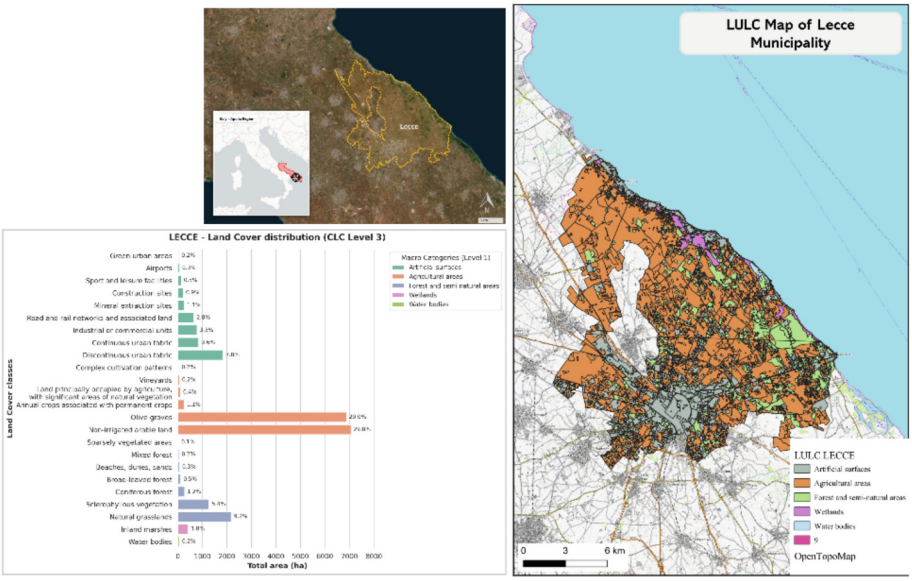

Fig. 1. The study area (Lecce, Southern Italy) and its land cover characterization based on the Corine Land Cover (CLC) nomenclature. The horizontal bars represent the total area (in hectares) occupied by each CLC Level 3 class, while the colors indicate the corresponding CLC Level 1 macro-categories.

3 Results

Although the methodological framework included a dual temporal scale (specifically, the analysis of individual daily acquisitions and the generation of a map representing the mean seasonal thermal anomaly), the processing from August 14, 2024, was selected to demonstrate the single-acquisition analysis. On this date, the study area recorded maximum air temperatures of 38.3 °C, a peak solar irradiance of 801.2 W/m2 and weak wind conditions mean wind speed: 1.1 m/s), following 23 consecutive days without precipitation.

The processed acquisitions reveal a spatial thermal inversion: contrary to the conventional Surface Urban Heat Island (SUHI) paradigm, the dense urban core maintained lower surface temperatures compared to the peri-urban and rural matrix, where the highest LST values were observed (see Fig. 2).

This trend is consistent with the analysis of diurnal LST dynamics for the city of Lecce, during the June - August period from 2018 to 2024 across six daily time intervals [46]. This phenomenon, found in other Mediterranean cities, is explained by the energy balance resulting from the rural characterization of Lecce: peri-urban soils, predominantly characterized by sparse vegetation, simple arable land in non-irrigated areas or sparse olive groves, present low thermal inertia and high exposure to direct radiation.

The frequency histogram provides an overview of the surface thermal regime of the surveyed area. The retrieved LST values span an overall range between approximately 34 °C and 55 °C.

The distribution exhibited a predominantly unimodal and slightly left-skewed behavior. The main peak occurred between 50 °C and 53 °C, indicating that these temperature ranges represent the dominant thermal condition within the landscape. The lower-temperature tail of the distribution represented a minority fraction of total pixels and spatially corresponded to coastal areas, wetlands, woodlands and the compact urban core. Conversely, the central portion of the distribution, encompassing most of the pixels, coincided with the peri-urban and rural matrix. The high frequency of elevated LST values reflects the summer physical conditions of exposed rural surfaces, including limited shading, direct solar exposure, low soil moisture availability and the widespread presence of bare soil.

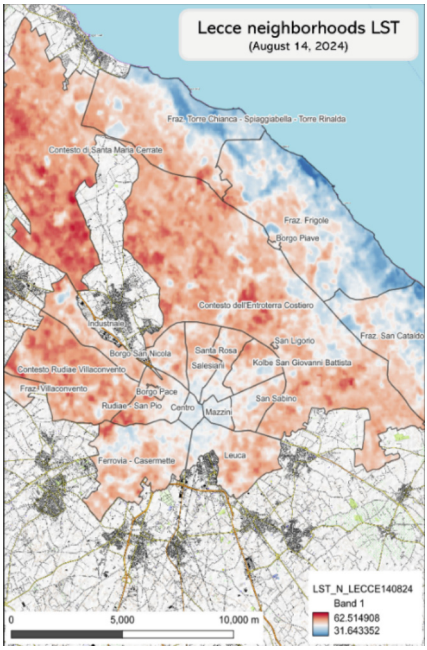

Fig. 2. Retrieved Land Surface Temperature (LST) for the municipality of Lecce (Landsat 8/9 acquisition, August 14, 2024; https://earthexplorer.usgs.gov/)

Quantifying the relative thermal anomaly (ΔT) required the definition of a rural thermal reference. For the spatial filtering procedure, an annular buffer between 5 and 10 km from the urban centroid was isolated, as this distance was considered sufficient to minimize the direct thermal influence of the urban core [47].

Utilizing Land Use Land Cover (LULC) vector data provided by the SIT Puglia portal (see Fig. 1, https://pugliacon.regione.puglia.it/web/sit-puglia-sit), the extraction was limited to vegetated classes (i.e., "Forest and semi-natural areas", "Wetlands" and "Agricultural areas"). A preliminary comparative analysis (see Fig. 3) revealed that specific agricultural classes ("non-irrigated arable land", "vineyards" and "olive groves") and semi-natural areas ("natural grasslands") recorded LST values exceeding the mean

(50.43 °C). Particular attention must be drawn to olive groves, which, alongside non-irrigated arable lands, constitute the most extensive land cover in the Lecce territory (accounting for 29% and 29.8%, respectively). The elevated LST values observed in these areas, despite their classification as vegetation cover, may be related to specific surface and canopy thermal dynamics. In olive groves, the satellite thermal signal represents a mixed radiometric response resulting from the combined contribution of the tree canopy and the exposed soil between rows. Under severe summer water stress conditions, potentially exacerbated by the effects of *Xylella fastidiosa*, the thermal contribution of bare and desiccated soil may become increasingly relevant within the emitted radiance signal. In the Lecce area, this interpretation is further supported by previous studies, as reported in [46], which analyzed summer soil moisture conditions between 2017 and 2022, reporting values frequently below 0.10 m^3/m^3, substantially lower than the average soil moisture levels typically observed across Italy (approximately 0.30 - 0.35 m^3/m^3). Consequently, these areas may behave as localized sources of sensible heat during daytime conditions.

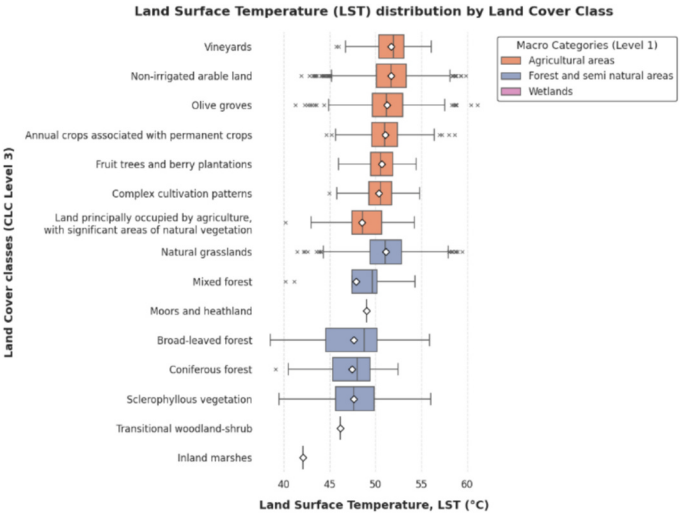

Fig. 3. Evaluation of vegetation cover (agriculture, forests and wetlands) for the rural baseline definition, highlighting the exclusion of agricultural surfaces with significant thermal anomalies.

The methodology adopted to define the rural reference value follows the approach described in [47] and consists of subtracting the mean LST value, calculated across a set of sampling points (pins) representative of non-urban areas, from each pixel within the study area. Each pin strictly satisfies the following spatial criteria:

1. it is the centroid of a union of contiguous Corine Land Cover (CLC) polygons belonging to the Level 1 macro-classes “Agricultural areas” or “Forest and semi-natural areas” or “Wetlands”;
2. it falls within the previously defined annular buffer;
3. it is located at a minimum distance of 350 m from the CLC “Artificial surfaces” class.

To isolate the rural thermal signal as accurately as possible, artificial surfaces and water bodies located within the annular buffer were explicitly excluded.

The LST spatial mean was calculated using a total of 3108 sample pins, obtaining a rural reference value LSTrif = 51.44 °C (median: 51.48 °C; SD: 2.59 °C; NMAD: 2.33 °C).

The thermal anomaly map was finally generated according to Eq. (2) [47, 48]:

$$\Delta T_{(x,y)} = LST_{(x,y)} - \overline{LST}_{rif} \tag{2}$$

where $\Delta T_{(x,y)}$ represents the thermal anomaly associated with the pixel located at coordinates (x,y).

The interpretation of thermal anomalies also considered the expected quality and uncertainty of the Landsat Collection 2 Level-2 Surface Temperature product. Landsat 8 TIRS and Landsat 9 TIRS-2 acquire thermal infrared data at a native spatial resolution of 100 m, subsequently resampled to 30 m in the distributed products and are characterized by high radiometric sensitivity. The sensors exhibit Noise Equivalent Delta Temperature (NE Δ T) values generally below 0.4 K and typically close to 0.1 K at 300 K under nominal operating conditions [23]. In addition, the operational USGS LST retrieval chain integrates atmospheric correction and ASTER GED emissivity information, leading to expected LST uncertainties generally on the order of 1–2 °C under clear-sky conditions [45]. Consequently, thermal anomalies substantially exceeding this uncertainty range can be interpreted as physically meaningful spatial signals rather than retrieval noise or instrumental artifacts.

Mapping the thermal anomaly (see Fig. 4) allowed the identification of two main thermal regimes:

- $\Delta T > 0$ defines hotspots areas, where the surface energy balance appears dominated by radiative absorption and reduced evaporative dissipation. This class includes peri-urban areas with bare soil/arable land in non-irrigated areas, olive groves, abandoned settlements and industrial zones (see Fig. 5).
- $\Delta T < 0$ indicates cool spot areas, where surface temperatures remain below the rural thermal reference. This class includes the dense historic center, urban green spaces (see Fig. 5), woodlands and wetlands.

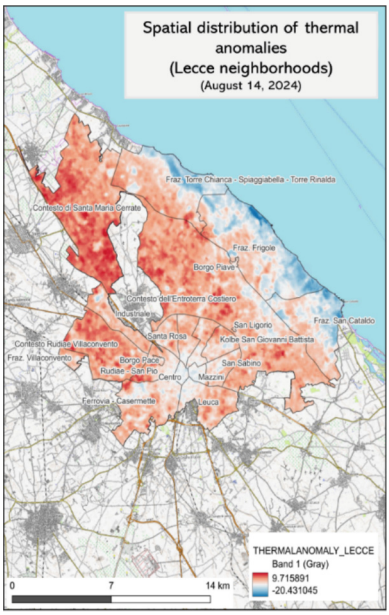

Fig. 4. Relative thermal anomaly map (ΔT) for the municipality of Lecce

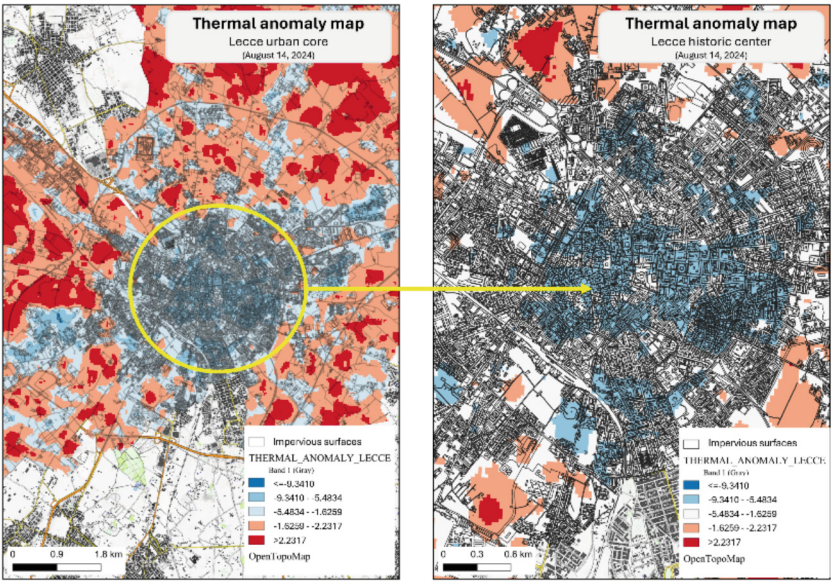

Fig. 5. Characterization of the Surface Urban Cool Island (SUCI) phenomenon, highlighting the negative thermal gradient associated with shaded impervious surfaces in the historic center and arboreal vegetation compared to the peri-urban agricultural context.

An interpretation of the cooling patterns observed within the urban core may be attributed to the combined effect of building shadows and urban geometry, characterized by high building height-to-street width ratios and reduced Sky View Factor (SVF) values [50, 51]. During the morning hours, this configuration maximizes street shading and prevents air mixing within urban canyons. Furthermore, the "Lecce Stone" (Miocene calcarenite rock) and the light-colored paving materials contribute to relatively high thermal inertia and medium-to-high albedo conditions. As a result, a fraction of incoming solar radiation is reflected, while surface heating occurs more gradually than in the surrounding rural environments. At the Landsat overpass time (approximately 11:30 local time), the city remains within its thermal accumulation phase and has not yet reached the afternoon thermal emission peak. Conversely, the surrounding peri-urban areas, characterized by lower thermal capacity and reduced soil moisture availability, tend to heat more rapidly under intense solar forcing.

This interpretation is consistent with the findings reported in [46], where the analysis of LST dynamics across different Local Climate Zones (LCZs) and six daily temporal intervals revealed a characteristic bell-shaped thermal curve. Minimum LST values were observed during the nighttime and early morning periods (23:00–03:00 and 03:00–06:00), whereas maximum temperatures occurred between 11:00 and 14:00. During this peak thermal interval, the compact urban core (classified as LCZ 2) exhibited lower LST values compared to peri-urban zones classified as LCZ 6 and LCZ 8. However, the study did not specifically investigate the thermal behavior of non-urban rural surfaces such as olive groves, bare soils, and wetlands.

Densely vegetated areas, including woodlands, irrigated urban parks and wetlands, are distinctly differentiated from both urban and semi-arid agricultural environments, representing actual climate mitigation zones (Fig. 6). In these areas, the climate mitigation mechanism is governed by the distribution of net radiation in favor of the latent heat flux. Vegetation dissipates the incident radiation through evapotranspiration: thermal energy is not stored in the soil or reflected; rather, it is absorbed to allow the state change from liquid to vapor. This process removes sensible heat from the environment, keeping the surface temperature close to air temperature and ensuring a fundamental ecosystem service of local thermoregulation.

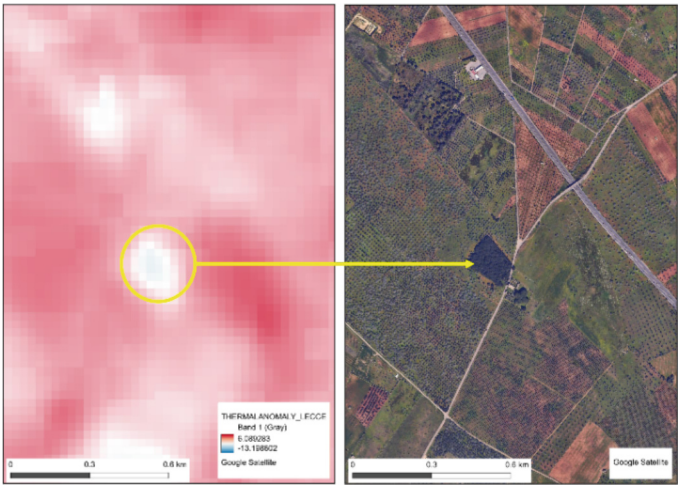

Fig. 6. Thermal heterogeneity of vegetation cover. Note how the olive grove, characterized by inter-row bare soil and direct exposure, acts as a Hotspot ($\Delta T > 0$), whereas the dense tree cover generates a cool spot ($\Delta T < 0$)

The thermodynamic drivers governing both the SUHI effect and the thermal anomalies associated with degraded agricultural soils are linked to similar radiative and hydrological imbalances. The transition from healthy vegetated surfaces to impervious urban materials or degraded semi-arid soils may significantly reduce evaporative cooling capacity by suppressing evapotranspiration processes. Under these conditions, a larger fraction of incoming radiative energy is converted into sensible heat fluxes rather than latent heat [15, 50, 52].

In urban environments, replacing natural surfaces with mineral materials generally increases heat storage capacity and modifies the optical and thermophysical properties of the surface. The relatively high thermal inertia of urban materials contributes to delayed heat release and plays a major role in sustaining the nocturnal SUHI effect [9].

Similarly, degraded rural environments characterized by bare soils, sparse vegetation and chronic summer water deficits may undergo rapid daytime surface heating due to low soil moisture availability and reduced thermal buffering capacity. In the Lecce context, these conditions appear particularly evident in agricultural areas affected by prolonged drought stress and vegetation degradation processes, including those associated with *Xylella fastidiosa*. These findings suggest that the degradation of vegetative cover may significantly amplify local microclimatic thermal extremes under semi-arid summer conditions.

Applying zonal statistics to the neighborhoods and hamlets of the city of Lecce enabled the quantification of the average thermal anomaly for each territorial unit (see Fig. 7).

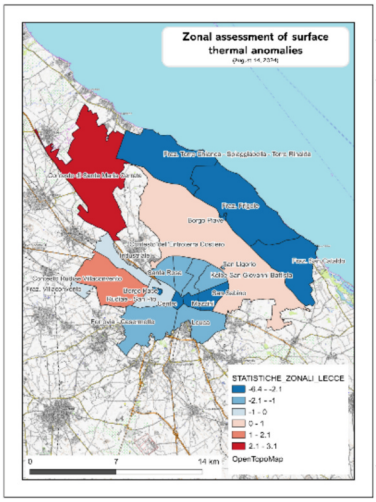

District	ΔT(°C) Mean	ΔT(°C) Median	ΔT(°C) Std. Dev.	ΔT(°C) Min
Fraz. Frigole	-6.39	-6.18	4.50	-20.66
Centro	-5.81	-5.78	0.82	-9.11
Fraz. San Cataldo	-5.45	-4.89	4.19	-18.40
Mazzini	-5.44	-5.68	1.56	-8.37
Fraz. Torre Chianca - Spiaggiabella - Torre Rinalda	-3.88	-2.62	5.16	-17.57
Borgo Piave	-3.12	-3.17	0.86	-4.74
Borgo Pace	-2.34	-2.37	1.41	-5.81
San Sabino	-2.12	-2.18	2.34	-8.06
Salesiani	-2.08	-2.51	2.64	-8.21
San Ligorio	-2.03	-2.05	0.93	-3.50
Kolbe San Giovanni Battista	-1.77	-2.10	2.96	-9.58
Ferrovia - Casermette	-1.57	-1.72	2.82	-9.49
Leuca	-1.47	-1.61	2.78	-7.91
Santa Rosa	-1.40	-1.26	2.42	-8.04
Borgo San Nicola	-1.07	-1.31	2.13	-7.31
Fraz. Villaconvento	-0.86	-0.97	2.40	-7.12
Rudiae - San Pio	-0.80	-1.43	3.35	-6.72
Industriale	-0.64	-0.57	2.43	-11.11
Contesto dell'Entroterra Costiero	0.62	0.86	2.75	-11.96
Contesto Rudiae Villaconvento	2.10	2.31	2.29	-7.18
Contesto di Santa Maria Cerrate	3.15	3.30	2.51	-6.97

Fig. 7. Quantification of the thermal regime at the neighborhood scale: mapping of the average anomaly calculated via zonal statistics, highlighting the heterogeneity between the urban core, coastal hamlets and peri-urban areas.

Tabular data analysis reveals two macro-clusters with opposite thermal behaviour:

1. Urban and natural cool spots (with negative thermal anomaly). These two types of territorial fabric share negative anomaly values but differ in physical cooling drivers:
   a. dense urban core: historic and commercial neighbourhoods show marked negative anomalies, with the historic center (ΔT_{mean} = -5.81 °C; ΔT_{median} = -5.78 °C; ΔT_{SD} = 0.82 °C) and the Mazzini neighbourhood (ΔT_{mean} = -5.44 °C; ΔT_{median} = -5.68 °C; ΔT_{SD} = 1.56 °C) being among the coolest areas overall. This evidence confirms the hypothesis of shading and the thermal inertia of materials as the dominant mitigating factors during the morning satellite acquisition hours.
   b. Coastal districts and wetlands: the lowest value was recorded in the district of Frigole (ΔT_{mean} = -6.39 °C; ΔT_{median} = -6.18 °C; ΔT_{SD} = 4.50 °C), followed by San Cataldo (ΔT_{mean} = -5.45 °C; ΔT_{median} = -4.89 °C; ΔT_{SD} = 4.19 °C) and the hamlet of Torre Chianca (ΔT_{mean} = -3.88 °C; ΔT_{median} = -2.62 °C; ΔT_{SD} = 5.16 °C). The low thermal regime is attributable to the presence of natural surfaces with high evaporative capacity (reservoirs, wooded areas of the Rauccio Park and the Le Cesine wetland) as well as the mitigating effect of the sea, given the areas' proximity to the coastline.
2. Peri-urban hotspots (with positive thermal anomaly). The highest surface temperature values are found in the Santa Maria Cerrate rural area (ΔT_{mean} = + 3.15 °C; ΔT_{median} = + 3.30 °C; ΔT_{SD} = 2.51 °C), Rudiae-Villaconvento (ΔT_{mean} = + 2.10 °C; ΔT_{median} = + 2.31 °C; ΔT_{SD} = 2.29 °C) and in the coastal hinterland area (ΔT_{mean} = + 0.62 °C; ΔT_{median} = + 0.86 °C; ΔT_{SD} = 2.75 °C). These areas confirm the thermal vulnerability of peri-urban surfaces characterized by bare soils, sparse vegetation under water stress, or large, unshaded, sealed areas, where the surface energy balance is heavily skewed toward sensible heat fluxes.

In temperate regions, urban areas are typically surrounded by densely vegetated rural landscapes. In this scenario, the city appears warmer than the countryside both day and night due to the lower evaporative cooling capacity of impervious surfaces compared to the rural environment.

Conversely, in strictly arid regions where urban grids border barren land, a diurnal gradient reversal is common. The city acts as an 'urban oasis,' maintaining localized humidity and lower surface temperatures through irrigated green spaces and geometric shading. Rapid nocturnal cooling of rock, however, contrasts with the thermal retention of urban concrete, driving a nighttime SUHI.

4 Discussion

The LST analysis in the Lecce municipal area, during the summer of 2024, highlights a thermal behaviour deviating from the classic SUHI paradigm. Processing the Landsat images, acquired at 11:30 local time, displays an inversion of the urban-rural thermal gradient: the compact urban core is, on average, cooler than the surrounding peri-urban agricultural matrix.

The average rural reference LST, calculated by applying spatial filtering to land cover classes and excluding thermally anomalous surfaces, is 51.44 °C, with peaks reaching 59.78 °C. The historic center and the most compact urban neighbourhoods show lower LSTs compared to the average rural LST, up to approximately -5.8 °C.

A morning SUCI, dominated by sensible heat flux, is therefore demonstrated for the area under study, functioning as a semi-arid area, although it is not classified as a semi-arid climate with traditional climate indices [32].

Beyond standard urban climate assessments, this finding holds implications for agricultural landscape management. The empirical evidence suggests that the desertification risk identified for this area [53] is driven more by localized soil overheating than by broad meteorological climate indices.

This data is crucial for agricultural land management because the organic matter contained in soil exposed directly to intense summer solar radiation (and consequently overheated, as demonstrated in the case study) is mineralized and leads to the depletion of soil fertility.

The spatial organization of the thermal regime, described by the map of thermal anomalies detected (ΔT), is divided into two main configurations:

– *Urban and natural cool spots ($\Delta T < 0$).* This behavior is attributable to urban morphology and material properties. Although the spatial average for the entire Lecce urban area indicates an open fabric (mean SVF of 0.96 and AR of 0.08 due to extensive green spaces and expanding peripheral zones [49]), the specific microclimate of the historic core follows a completely different dynamic. The Lecce historic fabric, comparable to the "compact midrise" Local Climate Zone, is characterized by narrow streets and locally high height-to-width (H/W) ratios. This specific micro-geometry creates mutual shading and lowers the local SVF, preventing daytime convective mixing. This factor, combined with the high thermal inertia and the local stone albedo, drives the daytime cooling effect.

– *Peri-urban and rural hotspots ($\Delta T > 0$).* Positive anomalies are concentrated mainly in the peri-urban and rural matrix, in areas characterized by bare soil, non-irrigated crops and sparse olive groves. In these contexts, numerous synergistic factors combine, all converging towards soil warming:

  - these soils generally exhibit a low albedo, increasing shortwave radiation absorption. Coupled with sparse vegetation cover, the exposed topsoil absorbs direct solar radiation, driving intense and rapid surface heating. Not even olive groves show a significant effect on this phenomenon in the Landsat thermal signal, which is evidently dominated by the bare soil temperature;
  - reduced soil moisture severely limits evapotranspiration and, therefore, prevents latent heat extraction.

The overall effect is a rapid accumulation of radiative energy across these exposed peri-urban and agricultural surfaces, which helps explain the elevated LST values observed in the Landsat acquisitions. Under late-morning summer conditions, these environments may therefore behave as dominant daytime heat sources relative to the compact urban core. At the very least, the results provide experimental evidence of a daytime SUCI effect, highlighting a substantial deviation from the classical SUHI paradigm traditionally associated with Mediterranean cities.

These findings suggest that urban thermal regimes in Mediterranean transitional environments cannot be interpreted exclusively through the conventional SUHI framework, but should instead be examined within a broader surface energy balance perspective that also incorporates processes related to land degradation, soil moisture depletion and semi-aridification of peri-urban agricultural landscapes.

From a territorial planning perspective, this evidence highlights the importance of considering urban and rural systems as strongly interconnected components of a single environmental and climatic framework, rather than as separate sectors analyzed independently. In the case of the Apulia region, this assumption has particularly relevant implications for the Regional Territorial Landscape Plan (PPTR) [54]. In particular, the present results:

1. provide empirical support for innovative territorial governance frameworks, such as the "*Patto Città-Campagna"* and the development of local ecological networks, reinforcing the need for integrated urban–rural planning strategies;
2. demonstrate how satellite-derived thermal analysis can offer an operational methodology for guiding climate-sensitive green infrastructure planning across multiple spatial scales, including urban, peri-urban and rural environments.

5 Conclusion

The empirical evidence presented in this study indicates that peri-urban agriculture plays a key role in the surface energy balance of the urban system. Although the present analysis focuses on the specific case of Lecce, the observed thermal dynamics may show potential transferability to other Mediterranean (Csa) urban environments characterized by compact settlements surrounded by semi-arid agricultural landscapes vulnerable to

land degradation processes. Under these conditions, sustainable soil management, the preservation of vegetative cover and the protection of wetlands and forested areas represent fundamental components for local thermoregulation. From a territorial planning perspective, these findings highlight the strategic importance of integrating peri-urban agricultural regeneration within broader climate adaptation policies. In particular, reducing bare soil exposure and restoring vegetative cover may contribute significantly to mitigating summer thermal stress and strengthening climate resilience in Mediterranean urban regions.

Acknowledgments. This study was funded by PRIN_EO4DES Earth Observation for Desertification, Italian University Ministry.

Disclosure of Interests. The authors have no competing interests to declare that are relevant to the content of this article.

References

1. Li, K., Chen, Y.: Identifying and characterizing frequency and maximum durations of surface urban heat and cool island across global cities. Sci. Total Environ. **859**, 160218 (2023)
2. Stewart, I.D.: A systematic review and scientific critique of methodology in modern urban heat island literature. Int. J. Climatol. **31**(2), 200–217 (2011)
3. Jiang, D., Wang, K.: The role of satellite-based remote sensing in improving simulated streamflow: a review. Water **11**(8), 1615 (2019)
4. Voogt, J.A., Oke, T.R.: Thermal remote sensing of urban climates. Remote Sens. Environ. **86**(3), 370–384 (2003)
5. Weng, Q., et al.: Estimation of land surface temperature–vegetation abundance relationship for urban heat island studies. Remote Sens. Environ. **89**(4), 467–483 (2004). https://doi.org/10.1016/j.rse.2003.11.005
6. Abedrabboh, O., Alfarra, M.R., Al-Ansari, T., Fountoukis, C.: Enhancing human thermal comfort in hot arid cities: a systematic review of urban heat island observations and mitigation strategies. Build. Environ. **283**, 113398 (2025)
7. Guo, F., et al.: Surface energy balance-based surface urban heat island decomposition at high resolution. Remote Sens. Environ. **315**, 114447 (2024)
8. ISPRA, Atlante 2025. Territori in trasformazione. https://www.isprambiente.gov.it/public_files/ATLANTE-2025-TERRITORI-IN-TRASFORMAZIONE-12-05.pdf. Accessed 30 Mar 2026
9. Campiotti, C. A. et al.: Gli ecosistemi vegetali per la rigenerazione ecologica delle città (2021). https://hdl.handle.net/20.500.12079/61021. Accessed 30 Mar 2026
10. Amorim, M.C.C.T., et al.: Day and night surface and atmospheric heat islands in a continental and temperate tropical environment. Urban Climate. **38**, 100918 (2021)
11. Salvati, A., et al.: Climatic performance of urban textures: analysis tools for a Mediterranean urban context. Energy Build. **185**, 162–179 (2019)
12. Leone, A., et al.: Take advantage of the black swan to improve the urban environment. TeMA J. Land Use Mobil. Environ. 247–259 (2020)
13. Li, H., et al.: A new method to quantify surface urban heat island intensity. Sci. Total Environ. **624**, 262–272 (2018)
14. Liu, Z., et al.: Identification of surface urban heat versus cool islands for arid cities depends on the choice of urban and rural definitions. Sci. Total Environ. **951**, 175631 (2024)

15. Mohammad, P., Goswami, A.: Exploring different indicators for quantifying surface urban heat and cool island together: a case study over two metropolitan cities of India. Environ. Dev. Sustainabil. **25**(10), 10857–10878 (2023)
16. Liu, L., Zhang, Y.: Urban heat island analysis using the landsat TM data and ASTER data: a case study in Hong Kong. Remote Sens. **3**(7), 1535–1552 (2011)
17. Pappaccogli, G., et al.: Dynamics of urban heat island intensity in Lecce, Italy: seasonal, diurnal and heat wave influence. Bull. Atmos. Sci. Technol. **5**(1), 8 (2024)
18. Wang, J., Lu, L., Zhou, X., Huang, G., Chen, Z.: Spatio-temporal patterns and drivers of the urban heat island effect in arid and semi-arid regions of Northern China. Remote Sens. **17**(8), 1339 (2025)
19. Karimi Firozjaei, M.K., et al.: Forecasting spatiotemporal dynamics of daytime surface urban cool islands in response to urbanization in drylands: case study of Kerman and Zahedan Cities. Iran **16**, 23 (2024)
20. Tetali, S., Baird, N., Klima, K.: A multicity analysis of daytime Surface Urban Heat Islands in India and the US. Sustain. Cities Soc. **77**, 103568 (2022)
21. Wu, X., et al.: Investigating surface urban heat islands in South America based on MODIS data from 2003–2016. Remote Sens. **11**(10), 1212 (2019)
22. Chakraborty, T., et al.: On the land emissivity assumption and Landsat-derived surface urban heat islands: a global analysis. Remote Sens. Environ. **265**, 112682 (2021)
23. Jimenez-Munoz, J.C., et al.: Land surface temperature retrieval methods from landsat-8 thermal infrared sensor data. IEEE Geosci. Remote Sens. Lett. **11**(10), 1840–1843 (2014)
24. Jiang, Y., Lin, W.: A comparative analysis of retrieval algorithms of land surface temperature from landsat-8 data: a case study of Shanghai, China. IJERPH **18**(11), 5659 (2021)
25. Lal, R.: Soil carbon sequestration impacts on global climate change and food security. Science **304**(5677), 1623–1627 (2004)
26. Cao, C., et al.: Correlation analysis of the urban heat island effect and its impact factors in China. Huan Jing ke Xue= Huanjing Kexue **38**(10), 3987–3997 (2017)
27. IPCC, Desertification (2019). https://www.ipcc.ch/site/assets/uploads/sites/4/2019/11/06_Chapter-3.pdf. Accessed 30 Mar 2026
28. Miao, S., et al.: Heat wave-induced augmentation of surface urban heat islands strongly regulated by rural background. Sustain. Cities Soc. **82**, 103874 (2022)
29. IPBES, Summary for policymakers of the assessment report on land degradation and restoration of the Intergovernmental Science-Policy Platform on Biodiversity and Ecosystem Services (2018). https://files.ipbes.net/ipbes-web-prod-public-files/spm_3bi_ldr_digital.pdf. Accessed 30 Mar 2026
30. Petito, M., et al.: Modelling and mapping Soil Organic Carbon in annual cropland under different farm management systems in the Apulia region of Southern Italy. Soil Tillage Res. **235**, 105916 (2024)
31. Oke, T.R.: Canyon geometry and the nocturnal urban heat island: comparison of scale model and field observations. J. Climatol. **1**(3), 237–254 (1981)
32. EEA – European Environment Agency, Climate change adaptation in the agriculture sector in Europe. EEA Report No 4/2019. ISBN 978–92–9480–072–5. https://www.eea.europa.eu/publications/cc-adaptation-agrucilture. Accessed 30 Mar 2026
33. SNPA, Consumo di suolo, dinamiche territoriali e servizi ecosistemici. https://www.snpambiente.it/wp-content/uploads/rapporto_consumo_di_suolo_2025.pdf. Accessed 30 Mar 2026
34. Siddiqui, A., et al.: An urban climate paradox of anthropogenic heat flux and urban cool island in a semi-arid urban environment. Atmosphere **16**(2), 151 (2025)
35. Singh, S., Avtar, R., Jain, A.K., Alkhuraiji, W.S., Zhran, M.: Influence of land use/land cover dynamics on urban surface metrics in semi-arid heritage cities. Land **14**(9), 1834 (2025)
36. De Razza, S., et al.: Mapping urban heatwaves and islands: the reverse effect of Salento's "white cities." Front. Earth Sci. **12**, 1375827 (2024)

37. Firozjaei, M.K., et al.: Daytime surface urban heat island variation in response to future urban expansion: an assessment of different climate regimes. Remote Sens. **17**(10), 1730 (2025)
38. Dialesandro, J.M., Wheeler, S.M., Abunnasr, Y.: Urban heat island behaviors in dryland regions. Environ. Res. Commun. **1**(8), 081005 (2019)
39. Rasul, A., Balzter, H., Smith, C.: Diurnal and seasonal variation of surface urban cool and heat islands in the semi-arid city of Erbil, Iraq. Climate **4**(3), 42 (2016)
40. Gago, J.E., et al.: Effect of land use/cover changes on urban cool island phenomenon in Seville, Spain. Energies **13**(12), 3040 (2020)
41. Rasul, A., Balzter, H., Smith, C.: Spatial variation of the daytime Surface Urban Cool Island during the dry season in Erbil, Iraqi Kurdistan, from Landsat 8. Urban clim. **14**, 176–186 (2015)
42. Dadashpoor, H., et al.: Explaining the role of land use changes on land surface temperature in an arid and semi-arid metropolitan area with multi-scale spatial regression analysis. Environ. Monit. Assess. **196**(2), 124 (2024)
43. Roy, D.P., et al.: Landsat-8: science and product vision for terrestrial global change research. Remote Sens. Environ. **145**, 154–172 (2014)
44. USGS Landsat 8 Data Users Handbook 2019. https://www.usgs.gov/landsat-missions/landsat-8-data-users-handbook. Accessed 30 Mar 2026
45. USGS Landsat collection 2. https://pubs.usgs.gov/publication/fs20213002. Accessed 30 Mar 2026
46. Pappaccogli, G., et al.: Summer diurnal LST variability across local climate zones using ECOSTRESS data in Lecce and Milan. Atmosphere. **16**(4), 377 (2025)
47. Pappalardo, E.S., et al.: Mapping urban heat islands and heat-related risk during heat waves from a climate justice perspective: a case study in the municipality of Padua (Italy) for inclusive adaptation policies. Landsc. Urban Plan. **238**, 104831 (2023)
48. Oke, T.R.: City size and the urban heat island. Atmos. Environ. (1967) **7**(8), 769–779 (1973)
49. Esposito, A., et al.: Urban morphology and surface urban heat island relationship during heat waves: a study of Milan and Lecce (Italy). Remote Sens. **16**(23), 4496 (2024)
50. Oke, T.R.: The energetic basis of the urban heat island. Q. J. R. Meteorol. Soc. **108**(455), 1–24 (1982)
51. Scarano, M., Sobrino, J.A.: On the relationship between the sky view factor and the land surface temperature derived by Landsat-8 images in Bari, Italy. Int. J. Remote Sens. **36**(19–20), 4820–4835 (2015)
52. Giannaros, T.M., Melas, D.: Study of the urban heat island in a coastal Mediterranean City: the case study of Thessaloniki, Greece. Atmos. Res. **118**, 103–120 (2012)
53. INEA, Atlante Nazionale delle aree a rischio di desertificazione (2007). https://www.mase.gov.it/portale/documents/d/guest/atlante_desertificazione-pdf-1. Accessed 30 Mar 2026
54. Barbanente, A., Grassini, L.: Fostering transitions in landscape policies: a multi-level perspective. Land Use Policy **112**, 105869 (2022)